Properties of Carbonate-Containing Aluminum Hydroxide Produced by Precipitation at Constant pH

EDWARD C. SCHOLTZ *, JOSEPH R. FELDKAMP ‡, JOE L. WHITE ‡, and STANLEY L. HEM *x

Received May 2, 1983, from the *Departments of *Industrial and Physical Pharmacy and ‡Agronomy, Purdue University, West Lafayette, IN 47907. Accepted for publication July 19, 1983.

Abstract □ Carbonate-containing aluminum hydroxide was precipitated at constant pH at intervals of 0.5 pH units from pH 6 to 10 by pumping 0.5 M $AlCl_3$ into the reaction vessel at a constant rate of 2 mL/min and infusing 2 M Na_2CO_3 at a rate necessary to maintain the desired pH. The pH of precipitation affected both the particle size and the composition of the precipitate. The particle size of the precipitate decreased as the pH of precipitation was increased from 6 to 10. The precipitates formed between pH 7.5 and 9.5 contained crystalline sodium aluminum hydroxycarbonate (dawsonite) in addition to amorphous carbonate-containing aluminum hydroxide.

Keyphrases □ pH—precipitation, carbonate-containing aluminum hydroxide □ Aluminum hydroxide—carbonate containing, production by precipitation at constant pH

Many processes for the preparation of aluminum hydroxide have been reported (1). Examples of these processes include (*a*) slowly cooling a concentrated sodium aluminate solution (2, 3); (*b*) bubbling CO_2 through a concentrated sodium aluminate solution (4–6); (*c*) hydrolysis of aluminum alcoholates (7, 8) or amalgamated aluminum foil (8); and (*d*) neutralization of an aluminum salt solution with a base (9–11). Aluminum hydroxide for pharmaceutical use is often prepared by the neutralization of an aluminum salt solution with a base. Some of the important variables associated with this method include temperature, pH, agitation, method of addition, reactants, reactant concentration, and addition rate (6, 12–18).

Three methods have been utilized for neutralizing an aluminum salt with a base. The first method involves the addition of the aluminum salt to the base (15, 17–20) and is limited to batch processes. The high pH of the base is decreased by the addition of the aluminum salt until a specific pH end point is reached. The second method is the opposite of the first, *i.e.*, base is added to the aluminum salt solution (12–14, 16–18, 21–23). The second method is also a batch process, as base is added until a specific pH end point is reached. In the third method, an aluminum salt solution and a base are simultaneously mixed (8, 17, 24). This method can be either a batch or a continuous process.

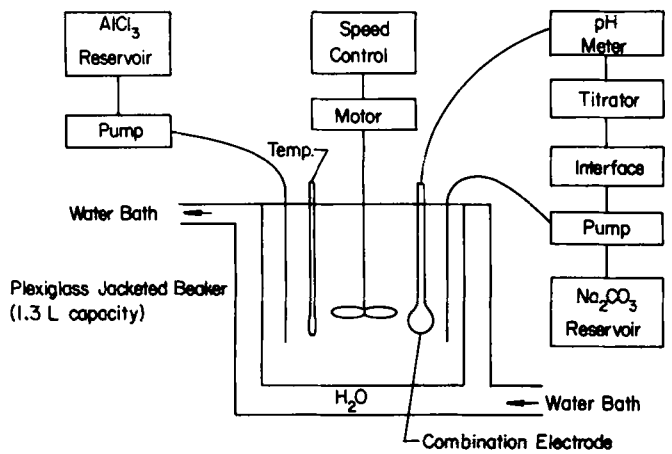

Figure 1—*Schematic of the apparatus used for constant pH precipitation of carbonate-containing aluminum hydroxide.*

Although far less common than other methods, the method of simultaneous mixing of reactants permits the precise control of pH. Since the solubility of aluminum hydroxide is very sensitive to pH, fixing this variable during the precipitation reaction should have a strong influence on the properties of the precipitate.

The objective of the present study was to examine aluminum hydroxide precipitates prepared under the constraint of constant pH. Precipitation reactions were carried out over the pH range of 6 to 10 with an automated apparatus which controls the pH within ±0.03 pH units of the desired value. Since carbonate-containing aluminum hydroxide is of considerable pharmaceutical importance (15), sodium carbonate was used as the base that was treated with aluminum chloride. After the precipitates were prepared, their physical and chemical properties were examined.

EXPERIMENTAL SECTION

Experimental laboratory gels were precipitated at 25°C from pH 6 to 10 at intervals of 0.5 pH units. The apparatus employed for the constant pH precipitations is shown in Fig. 1. The reaction vessel was a jacketed polymethyl methacrylate[1] beaker (10.2 cm i.d., 16.1 cm depth) with a capacity of 1.3 L. The vessel was fitted with four equally spaced polymethyl methacrylate baffles to provide efficient mixing.

The 0.5 M $AlCl_3$ and 2.0 M Na_2CO_3 solutions were injected into the reaction medium through submerged polytef tubes (0.1 mm i.d.). The aluminum chloride solution was pumped continuously into the reaction vessel at a constant rate of 2 mL/min. The sodium carbonate solution was infused into the system as needed to maintain the pH within 0.03 pH units of the predetermined value. The pH was constantly monitored and automatically controlled through the use of a titrator[2] linked between the pH meter and the sodium carbonate injection pump. The titrator was interfaced to the sodium carbonate pump with an opto-coupler chip.

A precipitation reaction was initiated by first placing 250 mL of 0.75 M $NaHCO_3$ into the reaction vessel. Since the pH was ~8.0, either 0.5 M $AlCl_3$ or 2.0 M Na_2CO_3 was infused until the desired pH was reached. When aluminum chloride was used, precipitation occurred during this period of pH adjustment, but the amount of precipitate formed was always insignificant when compared with the total amount of precipitate. Due to the large volume change occurring during the precipitation reaction (250 to 1300 mL), it was

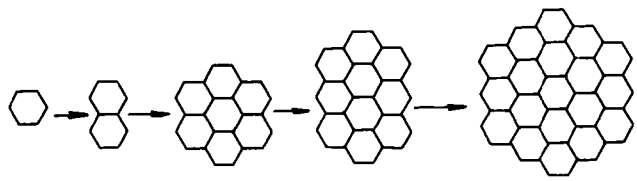

Figure 2—*Schematic of the development of crystalline aluminum hydroxide.*

[1] Plexiglas.
[2] PHM 62, TTT 60; Radiometer, Copenhagen, Denmark.

0022-3549/84/0700-0967$01.00/0

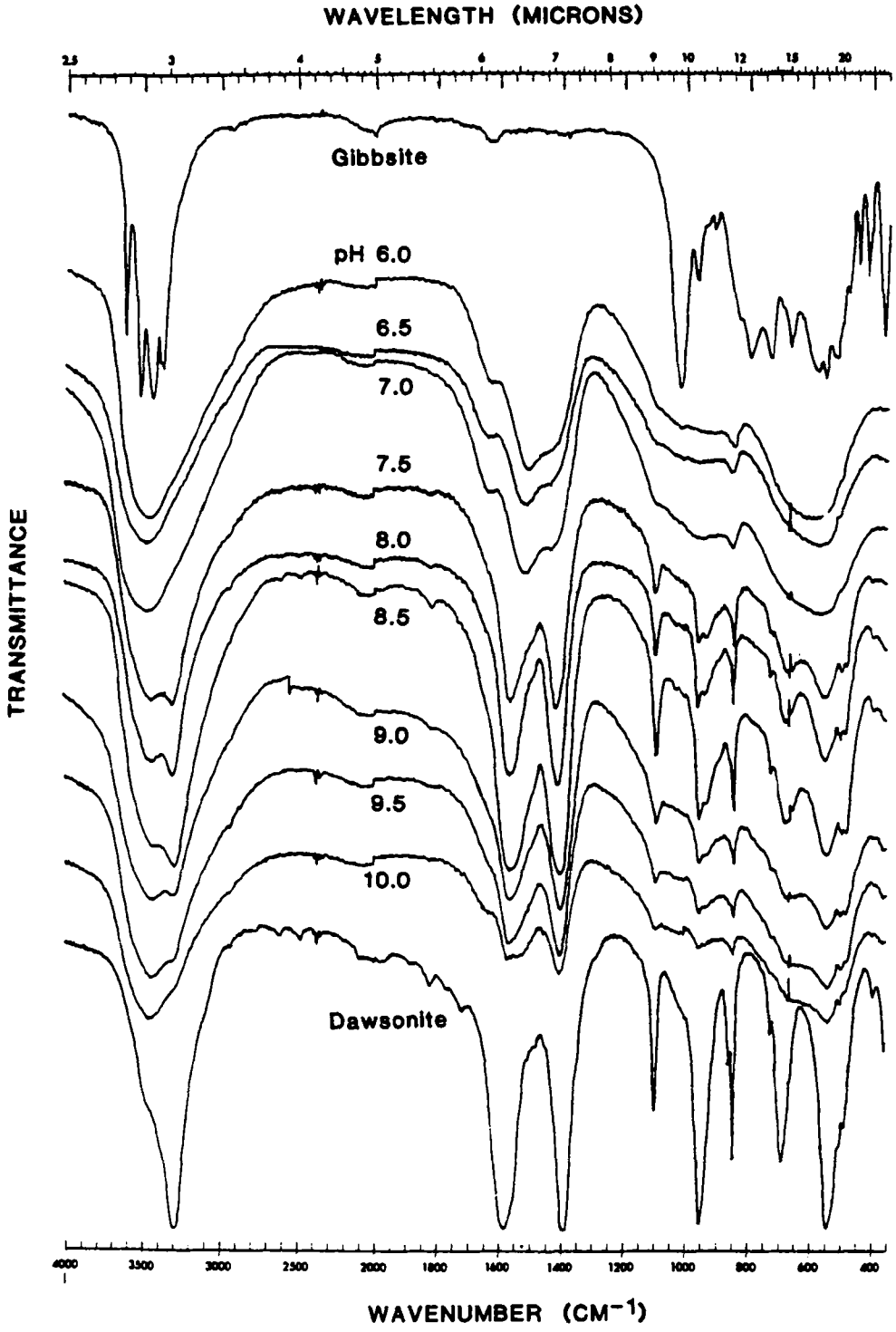

Figure 3—*IR spectra of precipitates formed at various pH_p.*

necessary to vary the stirring rate from 600 to 1200 rpm as needed. A marine propeller (diameter, 6.4 cm) was used to provide uniform mixing.

On completion of the precipitation reaction, the precipitate was washed by centrifugation with deionized water until the chloride content of the supernatant, as determined by a silver nitrate test, was $<6.2 \times 10^{-7}$ M. The washing step was always completed within 24 h of the termination of the precipitation reaction. The final suspension concentration was adjusted to fall within the range of 2–8% (w/w) equivalent Al_2O_3.

The equivalent aluminum oxide content was determined by chelatometric titration (25). IR analysis[3] was performed on air-dried samples as potassium bromide pellets (0.75 mg/300 mg of KBr). Carbonate was determined by a gasometric displacement technique (26, 27) with the Chittick apparatus[4]. The sodium ion content was measured by atomic absorption spectrometry[5]. The ability of magnesium cation to replace sodium cation in the pH 8.5 precipitate was determined by washing 600 mL of the precipitate with 600 mL of 1 M $MgCl_2$. The solids were washed four times with 1 M $MgCl_2$ by centrifugation and were then further washed with deionized water until the chloride content of the supernatant, as determined by a silver nitrate test, was $<6.2 \times 10^{-7}$ M. The point of zero charge (PZC) was determined for each sample by a continuous titration procedure (28).

To provide a qualitative measurement of particle size, the following sedimentation experiment was carried out. One hundred milliliters of sample was adjusted to the following conditions: 1% (w/v) equivalent Al_2O_3; ionic strength, 0.4; and pH = PZC. The sedimentation height in a sealed, undisturbed 100-mL graduated cylinder was monitored for 48 h. Two parameters

[3] Model 180; Perkin-Elmer Corp., Norwalk, Conn.
[4] Sargent Welch, Skokie, Ill.
[5] Model 290B; Perkin-Elmer Corp.

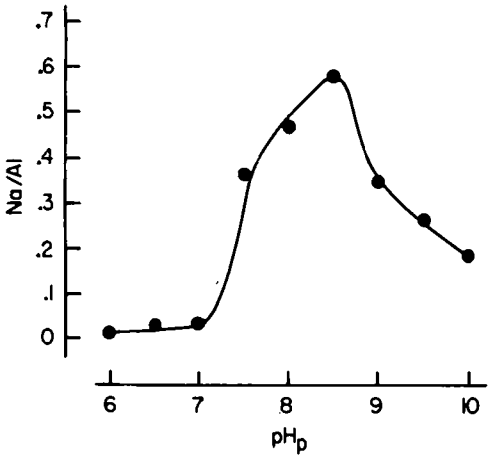

Figure 4—*Effect of pH_p on the sodium-aluminum molar ratio.*

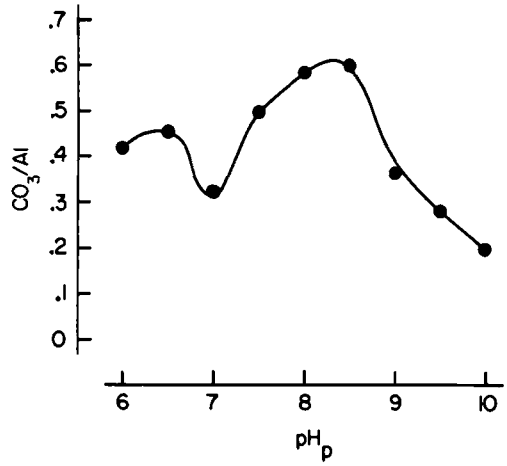

Figure 5—*Effect of pH_p on the carbonate-aluminum molar ratio.*

were used to summarize the sedimentation data: V_{48}, the sediment volume of the flocculated material at the end of the sedimentation period; and τ_{50}, the time required for the sediment volume to reach $(100 + V_{48})/2$. The values of both parameters are inversely related to particle size.

An additional qualitative measurement of particle size was the rate of acid neutralization as measured by pH-stat titration at pH 3.0 and 25°C (29). The time required to neutralize 50% of the sample, t_{50}, was used to characterize the rate of acid neutralization. A smaller value for t_{50} was assumed to infer a larger effective surface area and, hence, a smaller particle size. Particle size was directly measured for samples precipitated at pH 7.0 and 9.5 with a particle counter[6] and a fiber optic Doppler anemometer[7] (30), respectively.

RESULTS AND DISCUSSION

Chemical Structure—In a carbonate-containing system, X-ray and IR analyses have shown that aluminum hydroxide typically forms as an amorphous precipitate consisting of small, two-dimensional crystallites (primary particles) which vary widely in size (15, 31, 32). The crystallites have been identified as precursors of the various crystalline forms of aluminum hydroxide, such as gibbsite (32–34). The edges of the planar crystallites (Fig. 2) serve as sites for specific adsorption of carbonate, which likely takes place immediately after the crystallites have formed (15, 28, 31, 35).

The IR spectra of the precipitates formed at a pH of precipitation (pH_p) of 6.0, 6.5, and 7.0 (Fig. 3, Table I) are typical of amorphous aluminum hydroxide containing specifically adsorbed carbonate (15, 31) and indicate the presence of only an amorphous component. The precipitates formed between pH_p 7.5 and 9.5 exhibit a number of absorption bands in addition to the carbonate-containing aluminum hydroxide bands (Fig. 3). The new absorption bands correspond with the mineral dawsonite, a crystalline sodium aluminum hydroxycarbonate [$NaAl(OH)_2CO_3$] (Table I). The IR analysis indicates that the precipitate formed at pH_p 8.5 contained the largest fraction of dawsonite. This was confirmed by chemical analysis. The theoretical sodium-aluminum molar ratio for dawsonite is 1 and is typically near 0 for carbonate-containing aluminum hydroxide. The theoretical carbonate-aluminum molar ratio of dawsonite is 1, whereas the maximum carbonate-aluminum molar ratio of carbonate-containing aluminum hydroxide has been reported to be 0.5 (15). The maximum sodium-aluminum molar ratio (Fig. 4) and the maximum carbonate-aluminum molar ratio (Fig. 5) occurred at pH_p 8.5 and are attributed to dawsonite formation. Caution is required when interpreting the chemical analysis data since the sodium and carbonate ions do not reside exclusively in the dawsonite crystal lattice. Carbonate may be specifically adsorbed to the amorphous aluminum hydroxide component, and sodium can be bound in substantial quantities as a double-layer ion.

To more accurately determine the dawsonite content of the precipitate formed at pH_p 8.5, a portion of the precipitate was washed with 1 M $MgCl_2$ so that a magnesium-sodium cation exchange reaction might take place. Since the sodium in the dawsonite crystal lattice is not exchangeable, any nonexchangeable sodium is assumed to be associated with dawsonite. The sodium-aluminum molar ratio in carbonate-containing aluminum hydroxide-dawsonite systems can range from 0 in the absence of dawsonite to 1 in the absence of carbonate-containing aluminum hydroxide. The sodium-aluminum molar ratio of the precipitate at pH_p 8.5 decreased from 0.50 to 0.42 after magnesium exchange. The nonexchangeable sodium content indicates that dawsonite accounts for ~42% of the precipitate formed at pH_p 8.5.

The dawsonite content of the precipitate dropped sharply when the pH_p was above or below 8.5 (Figs. 3–5). For example, only trace levels of dawsonite were seen in the IR spectra at pH_p 10, and no indication of dawsonite was seen in the IR spectrum of precipitates at or below pH_p 7.0. Apparently, the requirements for the nucleation of dawsonite were best met at pH_p 8.5.

Particle Size—The rate of acid neutralization and sedimentation measurements can only be used to provide a qualitative measurement of particle size. However, since it was readily apparent from visual observation that the particle size was very sensitive to the pH_p, acid reactivity and sedimentation data were viewed as adequate for determining particle size trends as a function of pH_p. None of the three parameters was able to reflect the change in particle size over the entire pH_p range because of the substantial variation in particle size of the precipitates and the limitations of each technique. The rate of acid neutralization (Fig. 6) indicates a decrease in particle size from pH_p 6.0 to 7.5, whereas both sedimentation parameters, τ_{50} (Fig. 7) and V_{48} (Fig. 8), indicate a decrease in particle size from pH_p 7.0 to 10.0. However, when the t_{50}, τ_{50}, and V_{48} values are analyzed together, it is clear that the particle size decreases as the pH_p increases from 6 to 10.

Particle counter and fiber optic Doppler anemometer measurements were obtained for precipitates formed at pH_p 7.0 and 9.5 to confirm the conclusions drawn from the rate of acid neutralization and sedimentation studies. Particle size variation was quite large, so that measurements were made only for those samples precipitated at pH_p 7.0 and 9.5. The results indicated mean particle diameters of 12.0 and 0.20 μm at pH_p 7.0 and 9.5, respectively. Thus, over the pH_p range of 6.0 to 10.0, there is at least a 50-fold decrease in particle size.

Mechanism of Particle Size Variation—Although dawsonite was formed in significant quantities near pH_p 8.5, amorphous aluminum hydroxide formed the major component in all precipitates. Those precipitates formed at pH_p

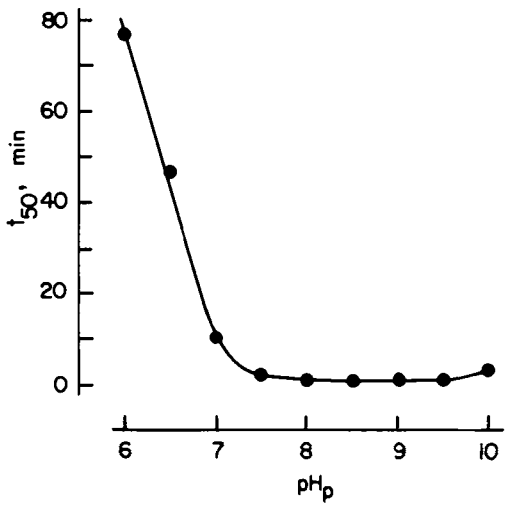

Figure 6—*Effect of the pH of precipitation on the time required to neutralize 50% of the theoretical acid (t_{50}) at pH 3 and 25°C.*

[6] Model TA II; Coulter Electronics, Inc., Hialeah, Fla.
[7] SIRA Institute, Ltd., Kent, England.

Table I—IR Absorption Bands of Precipitates Formed at Various pH_p

pH_p	Wave Number, cm^{-1}, and Assignment												
	O—H Stretching					Harmonic		Molecular H_2O	CO_3^{2-} Stretching				
Gibbsite[a]	3617	3520	3440	3390	3380			1630					
Dawsonite[b]						3285	1730		1570			1403	1100
Aluminum hydroxy-carbonate gel[c]			3440					1640		1500	1435		1090
6.0			3440					1625		1505	1435		1090
6.5			3460					1630		1505	1435		1095
7.0			3460					1630		1510	1435		1090
7.5			3430			3290			1560			1415	1093
8.0			3430			3290	1815		1560			1410	1093
8.5			3430			3290	1815		1560			1400	1093
9.0			3430			3290	1818		1560			1400	1093
9.5			3440			3290			1560			1400	1092
10.0			3440						1560			1403	1090

6.0, 6.5, 7.0, and 10.0 were found to be essentially free of dawsonite. Thus, the inverse relationship observed between pH_p and particle size is primarily related to the particle size variation of the amorphous component.

The lack of specific diffraction bands in the X-ray diffraction patterns of precipitates containing amorphous aluminum hydroxide establishes that there is no long-range atomic order in these systems (15, 31, 32, 40). The IR spectra (Fig. 3), which are much more sensitive to the presence of ordering, show broad hydroxyl-stretching bands centered at ~3440 cm^{-1}, which indicate the absence of specific proton environments. Thus, the observed large particles of amorphous carbonate-containing aluminum hydroxide (much larger than unit cell dimensions) must be composed of substantially smaller crystallites with dimensions not much larger than that of a unit cell, *i.e.*, primary particles.

The effect of the pH on the primary particle size is described by the von Weimarn law (41):

$$1/d = k(S/S_0) \qquad \text{(Eq. 1)}$$

where d is the diameter of the primary particle, k is a constant, S is the concentration of monomeric aluminum, and S_0 is the solubility, *i.e.*, the concentration of monomeric aluminum in equilibrium with infinitely large aluminum hydroxide particles, *e.g.*, highly crystalline gibbsite. The variable S is related to the concentration and infusion rate of the aluminum chloride solution. Since a 0.5 M $AlCl_3$ solution was infused into the reaction vessel at a rate of 2 mL/min for all precipitations, S is constant for all precipitates. The solubility of aluminum hydroxide (Fig. 9) is strongly influenced by pH (40, 42, 43), and therefore, S_0 varies considerably with pH_p. Since a 0.5 M $AlCl_3$ solution is infused into the reaction vessel, S/S_0 is always $\gg 1$. Therefore, precipitation is expected at all pH_p conditions.

The solubility of aluminum hydroxide is lowest at pH 5.5 to 6.0 and increases sharply as the pH is increased to 10. The ratio, S/S_0, is largest between pH 5.5 and 6.0 and decreases as the pH_p is increased. Therefore, the von Weimarn law predicts that the primary particle size is smallest near pH_p 6.0 and increases markedly as pH_p 10 is approached.

The von Weimarn law describes the size of the primary particles but does not provide any information about the subsequent formation of coagulates. However, based on the preceding conclusions concerning the primary crystallite size, DLVO theory may be used to predict the size of the coagulates. DLVO theory states that interparticle forces are a function of particle size (44, 45). In the case of electric double-layer repulsion between spherical particles of radius r, the following equation relates potential energy, V, to the separation distance, x, between two particles:

$$V = \epsilon\psi_0^2[r^2/(2r + x)]e^{-\kappa x} \qquad \text{(Eq. 2)}$$

where ϵ is the dielectric constant, ψ_0 is the surface electrical potential, and κ^{-1} is the Debye length. Clearly, the repulsive potential energy is increased for particles of larger radius. For large separation between particles, the potential energy is proportional to the square of the radius of the particles, so that the potential energy increases sharply as the particle size increases. The van der Waals attractive force, however, shows the same dependence on particle size, thereby compensating for the effect of particle size on the repulsive force (46).

Although particle size does not affect coagulation, the magnitude of the surface potential has a considerable effect which is independent of the van der Waals force. According to Eq. 2, the coulombic interaction energy varies with the square of the surface potential. For variable charge surfaces such as carbonate-containing aluminum hydroxide, ψ_0 is approximately proportional to PZC − pH (28, 47). Figure 10 shows that the difference between the PZC and the pH_p increases as the pH_p increases. The surface potential is therefore quite small for the precipitate formed at pH_p 6, but the surface potential becomes increasingly negative as the pH_p increases. Thus, the effect of surface potential on electric double-layer repulsion indicates that the probability of coagulation decreases as the pH_p increases from 6 to 10.

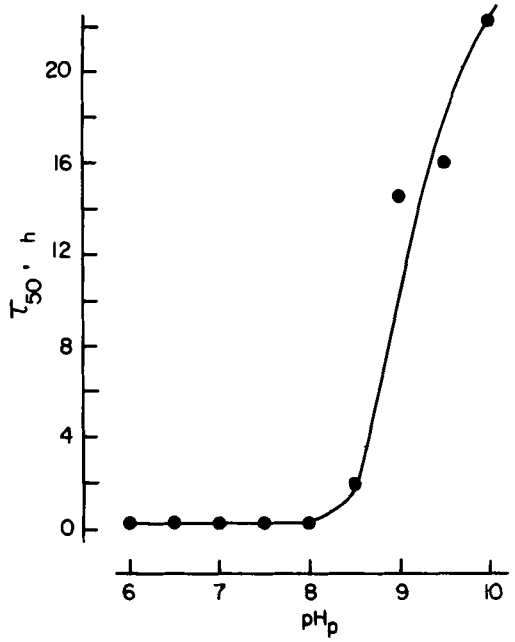

Figure 7—*Effect of pH_p on the sedimentation rate (T_{50}).*

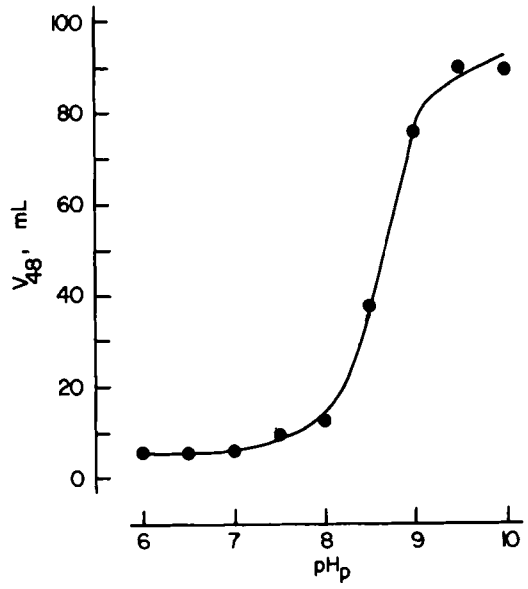

Figure 8—*Effect of pH_p on the sediment volume after 48 h (V_{48}).*

pH_p	Wave Number, cm^{-1}, and Assignment																	
	O—H Bending				CO_3^{2-} Bending		Miscellaneous[d]											
Gibbsite[a]	1025	965		910			800	740	667	585	560		515	476	450	420		
Dawsonite[b]			958	942	865	850		730	690			550	515	490				
Aluminum hydroxy-carbonate gel[c]						850				600								
6.0						848				580								
6.5						850				565								
7.0						850				565								
7.5			955	935		843		720	675			550		485				
8.0			955	935		843		727	673			550		482				
8.5			953	935		843		728	680			546		485				
9.0			952	935		842		723	670			546		480				
9.5			951			843						545						
10.0			950			843						540						

[a] References 36-38. [b] Reference 39. [c] Reference 31. [d] Including Al—O vibrations and CO_3^{2-} and O—H bending modes.

Once a coagulate has formed, its continued existence depends on its cohesive strength, which is a function of primary particle size. If only spherical particles are considered and the van der Waals attractive force is assumed to be the only interparticle force, then the following equation describes the relationship between coagulate cohesive strength, σ, the coagulate void volume fraction, ϕ, and the diameter of the primary particle, d:

$$\sigma = \frac{3(1-\phi)A}{64\phi a^2 d} \qquad \text{(Eq. 3)}$$

where A is a constant and a is the shortest interparticle separation distance (44). Equation 3 indicates that as ϕ, a, and d decrease (each decreases as the particle size decreases), the coagulate cohesive strength increases. The interparticle separation distance, a, is expected to be smaller for smaller particles due to a diminished absolute surface roughness. The coagulate void volume fraction, ϕ, decreases as the particle size, d, decreases due to packing considerations. Consequently, smaller primary particles are more likely to form survivable coagulates which are not easily destroyed when exposed to shear.

On consideration of the preceding factors, it is reasonable to conclude that the coagulate number (defined as the number of primary particles per coagulate) is largest for precipitates formed at pH_p 6 and considerably smaller for precipitates formed at pH_p 10. It is not certain, based solely on theoretical grounds, that there exists a sufficiently large variation in coagulate number to account for the greater than 50-fold variation in particle size observed by particle counter and fiber optic Doppler anemometry. However, the electric double-layer and coagulate cohesive strength considerations are of sufficient magnitude to account for the observed decrease in particle size as the pH_p is increased from 6 to 10.

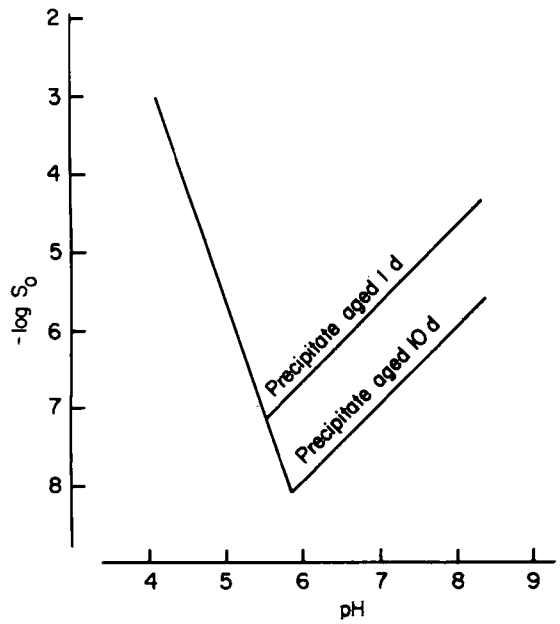

Figure 9—*Effect of pH on the solubility (S_0) of aluminum hydroxide (40).*

An excellent indication of the magnitude of the variation in coagulate number is provided by the pH-stat titrigrams for the precipitates formed at pH_p 6.0, 6.5, and 7.0 (Fig. 11). The titrigrams represent the cumulative amount of acid neutralized at pH 3 as a function of time. A very dramatic displacement of the titrigrams toward shorter reaction times is observed as the pH_p increases. If the von Weimarn law (Eq. 1) has correctly predicted that the primary particle size increases with increasing pH_p (which would tend to increase the t_{50}), then the observed increase in the rate of acid neutralization of the precipitate formed at pH_p 7.0 indicates a substantially lower coagulate number than the precipitate formed at pH_p 6.0.

Although speculative, the arrangement of primary particles within the secondary particles (coagulates) in carbonate-containing aluminum hydroxide might be comparable with the coagulate structures postulated for other materials composed of two-dimensional crystallites. The coagulate structure indicated in Fig. 12 has been proposed for carbon black (48). The edge-to-edge alignment of crystallites within the coagulates is in accord with the effects of van der Waals forces (49). The rectangular blocks represent the particles shown in Fig. 2 viewed from the edge. The results of this study suggest that such models might also describe the carbonate-containing aluminum hydroxide system.

Application to Commercial Precipitation of Carbonate-Containing Aluminum Hydroxide—The physical and chemical properties of carbonate-containing aluminum hydroxide are critically dependent on the pH_p. The property most sensitive to pH_p is particle size. The effect of pH_p on particle size is believed to be a result of variations in primary particle size as predicted by the von Weimarn law and the effects of double-layer repulsion and van der Waals attraction on coagulate formation (secondary particles). In addition to particle size effects, a crystalline phase identified as dawsonite, $NaAl(OH)_2CO_3$, was observed to form along with amorphous carbonate-containing aluminum hydroxide when the pH_p was between 7.5 and 9.5.

For most commercial aluminum hydroxide production, batch processes are utilized and, therefore, either lack pH control altogether or provide for very

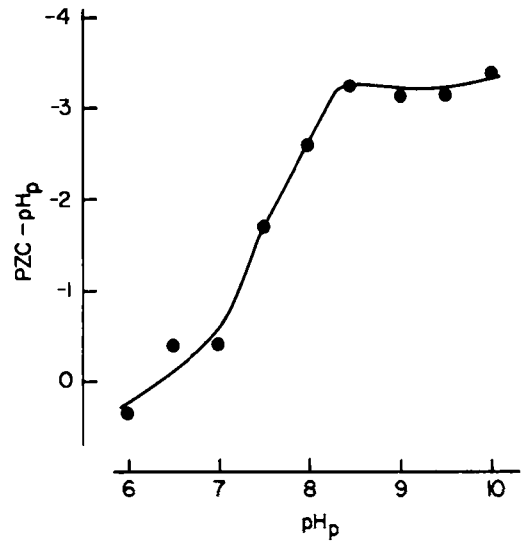

Figure 10—*Effect of pH_p on the difference between the point of zero charge (PZC) and pH_p.*

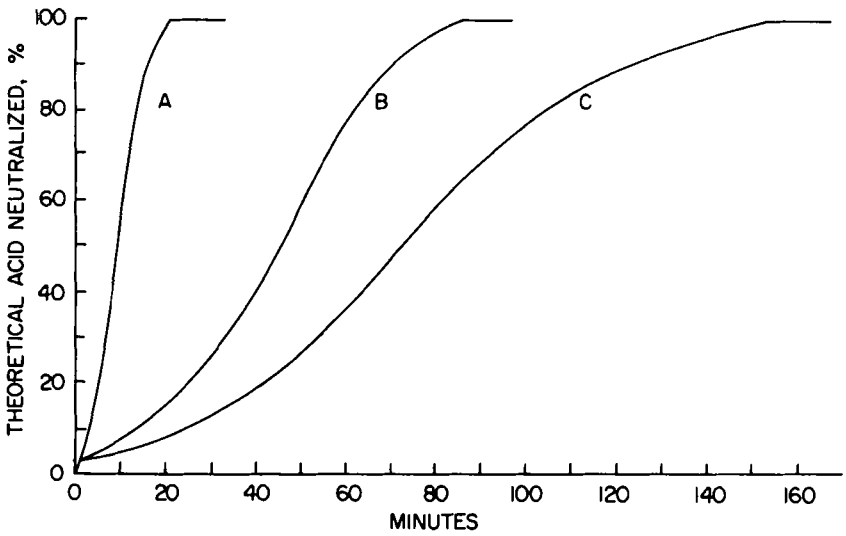

Figure 11—*Effect of pH_p on the rate of acid neutralization at pH 3.0 and 25°C. Key to pH_p: 7.0 (A); 6.5 (B); 6.0 (C).*

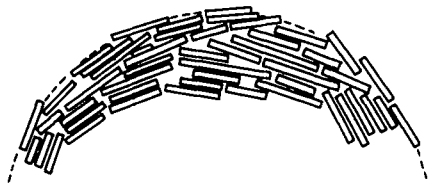

Figure 12—*Cross-sectional schematic for a coagulate (secondary particle) composed of planar primary crystallites (primary particles.)*

little control during the precipitation process. The product, therefore, is highly polydisperse and variable in composition. Consequently, considerable variation and uncertainty exist in the physical and chemical properties of carbonate-containing aluminum hydroxide precipitated by a batch process.

Certain properties may be desirable for specific applications of carbonate-containing aluminum hydroxide. The understanding gained from this study on the effect of the pH_p on the particle size and composition of the precipitate can be applied to aid in the design of precipitation processes which yield carbonate-containing aluminum hydroxides with desired properties. For example, a high surface area (small particle size) may be desired when aluminum hydroxide is used as an adsorbent. Thus, precipitation at a high pH is desired, as the smallest particle size was produced at pH_p 10.

In other situations, a low-viscosity suspension with a high solids content may be desired. To produce this property, a large particle size is necessary, and a pH_p of 6.0 is desirable. The precipitate at pH_p 6.0 formed a free-flowing suspension until a concentration of 18–20% (w/w) equivalent Al_2O_3 was reached, whereas the precipitate formed at pH_p 10 underwent gelation at only 2–3% (w/w) equivalent Al_2O_3. This behavior is readily recognized as a particle size effect since smaller particles are able to form a more extensive network or array (50).

It may also be desirable to produce carbonate-containing aluminum hydroxide which is free of sodium. The results of this study show that the precipitates formed between pH_p 7.5 and 9.5 contained appreciable amounts of dawsonite and, therefore, have a significant sodium content. The sodium in dawsonite cannot be removed through either washing or cation exchange since sodium is part of the crystal structure. Thus, batch precipitations which sweep through the pH_p range of 9.5 to 7.5 will produce precipitates which contain sodium as a permanent component.

REFERENCES

(1) B. C. Lippens and J. J. Steggerda, in "Physical and Chemical Aspects of Adsorbents and Catalysts," B. G. Linsen, Ed., Academic, New York, N.Y., 1970.

(2) V. D. Ponomarev, L. G. Romanov, and B. S. Dzhumabaev, Can. Patent No. 952,288 (1974) through *Chem. Abst.* **82,** 158321h (1975).

(3) T. Oku, K. Yamada, M. Yoshihara, and H. Kato, Japan. Kokai No. 74 04,696 (1974); through *Chem. Abst.*, **81,** 65717f (1974).

(4) J. Borska, G. Gawenda, E. Kosacka, R. Szmolke, J. Szylicki, and J. Ziembikiewicz, Pol. Patent No. 85,767 (1977); through *Chem. Abst.*, **90,** 61252p (1979).

(5) J. Matyasi, K. Nemeth, and L. Zsemberi, Fr. Demande No. 2,255,080 (1975); through *Chem. Abst.*, **84,** 184887h (1976).

(6) M. Popowicz, J. Berak, and A. Olechowska, *Przem. Chem.*, **51,** 607 (1972); through *Chem. Abst.*, **78,** 86598w (1973).

(7) C. J. Serna, J. L. White, and S. L. Hem, *Clays Clay Miner.*, **25,** 384 (1977).

(8) V. Alcvra, D. Ciomirtan, and M. Ionescu, *Rev. Roum. Chim.*, **17,** 1163 (1972).

(9) G. B. Glasscock, U.S. Patent No. 4,105,579 (1978); through *Chem. Abst.*, **90,** 76568v (1979).

(10) Barcroft Co., Neth. Appl. No. 7,806,135 (1979); through *Chem. Abst.*, **93,** 31788n (1980).

(11) Instituto de Biologia y Sueroterapia S.A., Span. Patent No. 428,760 (1977); through *Chem. Abst.*, **87,** 138017p (1977).

(12) T. Sato, *Z. Anorg. Allg. Chem.*, **391,** 69 (1972).

(13) A. C. Vermeulen, J. W. Geus, R. J. Stol, and P. L. DeBruyn, *J. Colloid Interface Sci.*, **51,** 449 (1975).

(14) C. J. Serna, J. L. White, and S. L. Hem, *J. Pharm. Sci.*, **67,** 1179 (1978).

(15) C. J. Serna, J. L. White, and S. L. Hem, *J. Pharm. Sci.*, **67,** 1144 (1978).

(16) S. L. Hem, E. J. Russo, S. M. Bahal, and R. S. Levi, *J. Pharm. Sci.*, **59,** 317 (1970).

(17) J. A. Lewis and C. A. Taylor, *J. Appl. Chem.*, **8,** 223 (1958).

(18) R. Soliman, *Pharmazie*, **29,** 62 (1974).

(19) Barcroft Co., Belg. Patent No. 867,982 (1978); through *Chem. Abst.*, **90,** 92439j (1979).

(20) C. A. Signorino and E. J. Wozinicki, Br. Patent No. 1,467,548 (1977); through *Chem. Abst.*, **87,** 69726e (1977).

(21) S. L. Nail, J. L. White, and S. L. Hem, *J. Pharm. Sci.*, **65,** 1255 (1976).

(22) S. L. Nail, J. L. White, and S. L. Hem, *J. Pharm. Sci.*, **65,** 1188 (1976).

(23) D. Papee, R. Tertian, and R. Biais, *Bull. Soc. Chim. Fr.*, **1958,** 1301.

(24) G. Drautzburg and E. Urmann, Ger. Offen. No. 1,921,999 (1970); through *Chem. Abst.*, **74,** 5113b (1971).

(25) "The United States Pharmacopeia," 20th rev., U.S. Pharmacopeial Convention, Rockville, Md., 1980, p. 25.

(26) "Official Methods of Analysis of the Association of Official Analytical Chemists," 12th ed., W. Horwitz, Ed., Assoc. of Official Analyt. Chemists, Washington, D.C., 1975, p. 147.

(27) E. C. Scholtz, Ph.D. Thesis, Purdue University, December 1981.

(28) J. R. Feldkamp, D. N. Shah, S. L. Meyer, J. L. White, and S. L. Hem, *J. Pharm. Sci.*, **70,** 638 (1981).

(29) N. J. Kerkhof, R. K. Vanderlaan, J. L. White, and S. L. Hem, *J. Pharm. Sci.*, **66,** 1528 (1977).

(30) D. A. Ross, H. S. Dhadwal, and R. B. Dyott, *J. Colloid Interface Sci.*, **64,** 533 (1978).

(31) C. J. Serna, J. L. White, and S. L. Hem, *J. Pharm. Sci.*, **67,** 324 (1978).

(32) S. L. Nail, J. L. White, and S. L. Hem, *J. Pharm. Sci.*, **64,** 1166 (1975).

(33) P. H. Hsu, in "Minerals in Soil Environments," J. B. Dixon and S. B. Weed, Eds., Soil Sci. Soc. of America, Madison, Wis., 1977, p. 120.

(34) P. H. Hsu and T. F. Bates, *Mineral. Mag.*, **33**, 749 (1964).
(35) C. J. Serna, J. L. White, and S. L. Hem, *Soil Sci. Soc. Am. J.*, **41**, 1009 (1977).
(36) L. D. Frederickson, *Anal. Chem.*, **26**, 1883 (1954).
(37) A. J. Leonard, F. Van Cauwelaert, and J. J. Fripiat, *J. Phys. Chem.*, **71**, 695 (1967).
(38) J. A. Gasden, "Infrared Spectra of Minerals and Related Inorganic Compounds," Butterworth, Reading, Mass., 1975, pp. 54, 74.
(39) A. J. Frueh and J. P. Golightly, *Can. Mineral.*, **9**, 51 (1967).
(40) J. D. Hem and C. E. Roberson, "Geological Survey Water-Supply Paper 1827-A," U.S. Government Printing Office, Washington, D.C., 1967 p. A47.
(41) A. W. Adamson, "Physical Chemistry of Surfaces," 3rd ed., Wiley, New York, N.Y., 1976, pp. 372-384.
(42) H. M. May, P. A. Helmke, and M. L. Jackson, *Geochim. Cosmochim. Acta*, **43**, 861 (1979).
(43) H. M. May, P. A. Helmke, and M. L. Jackson, *Chem. Geol.*, **24**, 259 (1979).
(44) Derjaguin, Landau, Vervey, and Overbeek (DLVO); A. Nakamura and R. Okada, *Colloid Polym., Sci.*, **254**, 497 (1976).
(45) H. van Olphen, "An Introduction to Clay Colloid Chemistry," 2nd ed., Wiley, New York, N.Y., 1977, p. 46.
(46) J. Mahanty and B. W. Ninham, "Dispersion Forces," Academic, New York, N.Y., 1976, p. 16.
(47) R. G. Gast, in "Minerals in Soil Environments," J. B. Dixon and S. B. Weed, Eds., Soil Sci. Soc. of America, Madison, Wis., 1977, pp. 36, 37.
(48) F. A. Heckman, *Rubber Chem. Technol.*, **37**, 1245 (1964).
(49) J. Mahanty and B. W. Ninham, "Dispersion Forces," Academic, New York, N.Y., 1976, pp. 21, 22.
(50) J. R. Feldkamp, J. L. White, and S. L. Hem, *J. Pharm. Sci.*, **71**, 43 (1982).

ACKNOWLEDGMENTS

This study was supported in part by William H. Rorer, Inc. This report is Journal Paper 9371, Purdue University Agricultural Experiment Station, West Lafayette, IN 47907. A preliminary report was presented at the Basic Pharmaceutics Section, Academy of Pharmaceutical Sciences, San Diego, Calif., November 1982.

Hypolipidemic Activity of Tetrakis-μ-(trimethylamine-boranecarboxylato)-*bis*(trimethylamine-carboxyborane)-dicopper(II) in Rodents and Its Effect on Lipid Metabolism

I. H. HALL *[x], W. L. WILLIAMS, Jr.*, COLLEEN J. GILBERT*, A. T. Mc PHAIL [‡], and B. F. SPIELVOGEL [‡]

Received April 25, 1983, from the **School of Pharmacy, University of North Carolina at Chapel Hill, Chapel Hill, 27514* and [‡]*Paul M. Gross Chemical Laboratory, Duke University, Durham, NC 27706.* Accepted for publication June 8, 1983.

Abstract □ A binuclear copper(II) complex was shown to have potent hypolipidemic activity in rats and mice at low doses, *i.e.*, 2.5-10 mg/kg/d. The agent moderately lowered liver ATP-dependent citrate lyase, acetyl CoA synthetase, and phosphatidate phosphohydrolase activities *in vivo*. The appetite of the animal was reduced by drug treatment, and orally administered cholesterol absorption from the intestine was markedly lowered. Higher lipid levels were found in the chyme and the feces, indicating accelerated excretion of lipids by the drug, probably *via* the biliary route. Organs, *e.g.*, liver and small intestine, as well as serum lipoprotein levels, demonstrated lower lipid content after drug administration. Thus, this chemical class of agents may have potential as a hypolipidemic agent in humans.

Keyphrases □ Binuclear copper(II) complex—antihyperlipidemic activity in rodents, effect on lipid metabolism □ Antihyperlipidemic agents—binuclear copper(II) complex, activity in rodents, effect on lipid metabolism □ Cholesterol—antihyperlipidemic effect of binuclear copper(II) complex

Recently, a series of amine-cyanoboranes and amine-carboxyboranes were observed to be hypolipidemic in mice between 5 and 20 mg/kg ip (1). From *in vitro* studies of these series, the ability to lower serum cholesterol appeared to correlate positively with the inhibition of the liver regulatory enzyme β-hydroxy-β-methyl glutaryl CoA (HMG CoA reductase) reductase activity, and the reduction of serum triglyceride was correlated with inhibition of fatty acid synthetase activity (1). Subsequently, a binuclear copper(II) complex derived from trimethylamine-carboxyborane, *viz.*, tetrakis-μ-(trimethylamine-boranecarboxylato)-*bis*(trimethylamine-carboxyborane)dicopper(II) was synthesized, and its effects on lipid metabolism is reported.

EXPERIMENTAL SECTION

Preparation of Tetrakis-μ-(trimethylamine-boranecarboxylato)-*bis*(trimethylamine-carboxyborane)dicopper(II)—Cupric chloride was purchased commercially[1]. Trimethylamine-carboxyborane was prepared as described previously (2). Trimethylamine-carboxyborane (1.8703 g, 15.9 mmol) was dissolved in 1 M NaOH (16 mL) and water (20 mL). Dropwise addition of 23 mL of a solution of $CuCl_2 \cdot 2H_2O$ (1.36 g, 8 mmol) in water (40 mL) produced a dark green solution which was allowed to stand overnight. Subsequent filtration through a fine-fritted funnel removed a greenish-brown sludge and left a dark-green filtrate, which was allowed to evaporate in the atmosphere. After 6 d, the solution evaporated, leaving many small green crystals in a clear liquor. These crystals were filtered and washed with chloroform (40°C); no $(CH_3)_3N \cdot BH_2COOH$ crystals were evident. The green crystals were then splashed with a minimal amount of cold water to ensure removal of any trace of sodium chloride and dried *in vacuo*. The yield was 0.49 g (23%), mp 165°C (dec.); IR: ν_{BH}, 2350, $\nu_{C=O}$ 1665 cm^{-1}.

Anal.—Calc. for $C_{24}H_{68}B_6Cu_2N_6O_{12}$: C, 34.95; H, 8.31; N, 10.19. Found: C, 35.00; H, 8.49; N, 10.15. The structure was determined by single-crystal X-ray analysis (3).

Antihyperlipidemic Screens in Normal Rodents—Compounds to be tested were suspended in 1% aqueous carboxymethylcellulose and administered to male CF_1 mice (~25 g) intraperitoneally for 16 d or male Holtzman rats (~350 g) orally by an intubation needle for 14 d. On days 9 and 14 or 16, blood was obtained by tail vein bleeding, and the serum was separated by centrifugation for 3 min. The serum cholesterol levels were determined by a modification of the Liebermann-Burchard reaction (4). Serum triglyceride levels were determined with a commercial kit[2] for a different group of animals bled on day 14 or 16.

Testing in Induced Hyperlipidemic Mice—Male CF_1 mice (~25 g) were

[1] Allied Chemicals, Morristown, N.J.
[2] Fisher, Hycel Triglyceride Test Kit.

0022-3549/84/0700-0973$01.00/0